

Luciferase and Luciferin Co-immobilized Mesoporous Silica Nanoparticle Materials for Intracellular Biocatalysis

Xiaoxing Sun, Yannan Zhao, Victor S.-Y. Lin,[†] Igor I. Slowing,^{*} and Brian G. Trewyn^{*}

Department of Chemistry, U.S. Department of Energy, and Ames Laboratory, Iowa State University, Ames, Iowa 50011-3111, United States

S Supporting Information

ABSTRACT: We report a gold nanoparticle (AuNP)-capped mesoporous silica nanoparticle (Au-MSN) platform for intracellular codelivery of an enzyme and a substrate with retention of bioactivity. As a proof-of-concept demonstration, Au-MSNs are shown to release luciferin from the interior pores of MSN upon AuNP uncapping in response to disulfide-reducing antioxidants and codeliver bioactive luciferase from the PEGylated exterior surface of Au-MSN to HeLa cells. The effectiveness of luciferase-catalyzed luciferin oxidation and luminescence emission in the presence of intracellular ATP was measured by a luminometer. Overall, the chemical tailorability of the Au-MSN platform to retain enzyme bioactivity, the ability to codeliver enzyme and substrate, and the potential for imaging tumor growth and metastasis afforded by intracellular ATP- and glutathione-dependent bioluminescence make this platform appealing for intracellular controlled catalysis and tumor imaging.

Intracellular delivery and controlled release of multiple biogenic molecules, such as genes, enzymes, proteins, and other molecules of pharmaceutical interest,^{1–5} provides a powerful tool for therapeutics and fundamental studies of biological processes such as enzyme-catalyzed reactions. While intracellular enzyme delivery has been studied using nanocarriers,^{2–4} the codelivery of enzyme and substrate for enzymatic reactions mediated by intracellular factors has not been reported to date. Modulation of enzymatic reactions by cellular factors provides a potent means to gain information about cellular processes such as signal transduction, DNA replication, and metabolism. These cellular factors can be considered as biological markers and therapeutic targets for disease diagnosis and treatment.^{6–8} For example, a key metabolite involved in maintaining a reduced intracellular redox milieu is the tripeptide glutathione (GSH).⁹ GSH has long been suggested to be part of signaling cascades transducing environmental signals to the nucleus, and its elevated concentration in many types of tumors is often associated with an increased resistance to chemo- and radiotherapy.⁸ Likewise, as biological energy, adenosine triphosphate (ATP) is involved in a multitude of important intracellular physiological processes, such as protein metabolism and cell apoptosis, the level of which is a measure of tumor cell viability and growth.⁶ Therefore, intracellular codelivery of enzymes and substrates for cellular factor (e.g., GSH and ATP)-mediated enzymatic reactions would not only afford novel biocatalysis inside live cells but also find application in monitoring of tumor growth and metastasis. Two major challenges,

however, are (1) the design of nanomaterials for intracellular controlled release of multiple biogenic species with preserved bioactivity and (2) the development of methods for imaging and quantification of cellular-factor-mediated catalytic reactions.

Mesoporous silica nanoparticles (MSNs) were recently demonstrated to be excellent candidates as vehicles for codelivery applications^{10,11} as a result of the coexistence of both interior pore and exterior particle surfaces for loading various guest molecules. This unique feature provides the possibility of using MSN for controlled release and codelivery of enzymes and substrates for intracellular enzymatic reactions. With respect to the challenge of imaging and quantification, most studies on nanoparticle-based tumor imaging have focused on their cellular uptake and have relied heavily on fluorescence readout, which cannot provide biologically relevant information on cellular processes. Bioluminescence has gained favor in the past decade as an attractive approach for tumor imaging.^{12–17} This technique is based on light emission by the luciferase-catalyzed oxidation of the luciferin substrate, which occurs in an ATP-dependent manner.^{18,19} A vast number of experiments have been carried out to examine tumor growth and the effect of therapeutics using tumor cell lines that have been genetically engineered to produce luciferase.^{12–17} However, the detection of photons is dependent on the circulatory half-life of the injected luciferin substrate and its perfusion into the tumor.²⁰ The fast elimination of luciferin from circulation makes utilizing it in many clinical applications challenging.²⁰ Both the sophisticated gene engineering and the short circulatory half-life of luciferin call for novel nanomaterials for intracellular codelivery of luciferase and luciferin, which would offer the additional advantage of improved tumor uptake via the enhanced permeability and retention (EPR) effect.²¹

Herein we report the development of a gold nanoparticle (AuNP)-capped MSN (Au-MSN) system and our investigations of the intracellular codelivery of luciferase and luciferin as a model enzyme–substrate pair. As depicted in Figure 1, luciferin is loaded in the mesopores of the MSNs and encapsulated with disulfide-linked AuNPs that physically block the luciferin from leaching out. Luciferase is physisorbed on the PEGylated external surface of the Au-MSNs through electrostatic interactions, as previously demonstrated.²² Luciferin molecules trapped inside the pores are released upon uncapping by intracellular disulfide-reducing antioxidants such as GSH or cysteine or the introduction of dithiothreitol (DTT).²³ The released luciferin is in turn converted by the codelivered luciferase to oxyluciferin in the

Received: August 24, 2011

Published: October 18, 2011

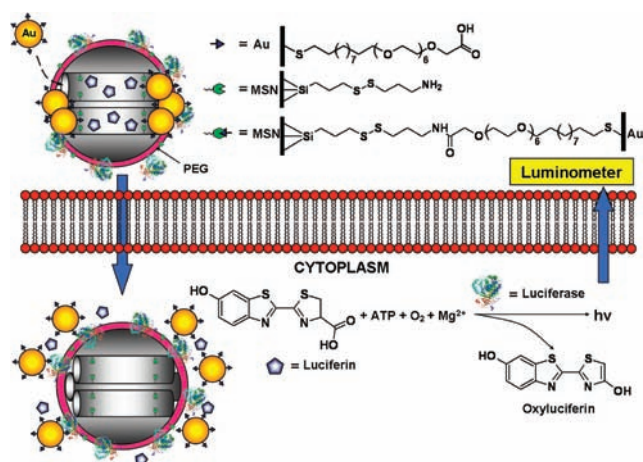


Figure 1. Schematic representation of Au-MSNs for intracellular codelivery of luciferase and luciferin.

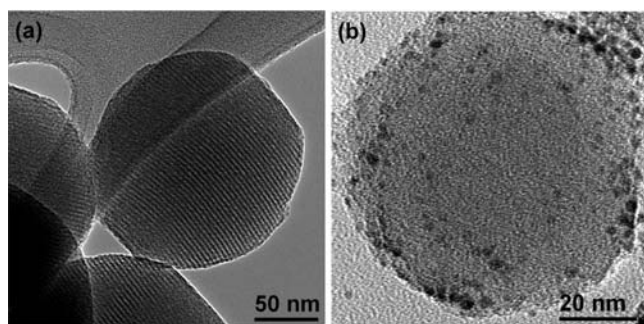


Figure 2. TEM images of (a) PEGylated linker-MSNs and (b) a luciferin-loaded Au-MSN. A high-magnification image of a luciferin-loaded Au-MSN is shown in Figure S3d.

presence of intracellular ATP and cofactor Mg²⁺, along with the release of energy in the form of photons that can be measured with a luminometer.

We first synthesized a 3-(propyldisulfanyl)ethylamine (0.9 mmol g⁻¹)-functionalized mesoporous silica nanosphere (linker-MSN) material using our previously reported method.^{23,24} As described in the Supporting Information (SI), the material was PEGylated by grafting 2-[methoxy(polyethylenoxy)propyl]trimethoxysilane to yield the PEGylated (0.1 mmol g⁻¹) linker-MSN with an average particle diameter of 160 nm and an MCM-41-type channel-like mesoporous structure (BJH pore diameter = 2.5 nm) (Figure 2a).

We then functionalized the surface of the AuNPs with a carboxylic acid-terminated poly(ethylene glycol) (PEG) linker (Figure 1) through exchange of 1-propanethiol-protected AuNPs²⁵ with PEG-functionalized thiol ligands in dichloromethane (see the SI). The PEG-functionalized AuNPs (PEG-AuNPs) were negatively charged (ζ potential = -39.6 mV) in PBS (pH 7.4) with an average particle diameter of 3 nm, as determined by transmission electron microscopy (TEM) (Figure S3b in the SI).

Before the enzyme–substrate Au-MSN system was constructed, the influence of MSNs and AuNPs on the enzymatic activity of luciferase was analyzed by means of a luciferase activity assay.^{26,27} As shown in Figure S4, the luciferase activity was depressed dramatically upon incubation with linker-MSNs and 1-propanethiol-stabilized AuNPs, with activities of ~20 and <15%, respectively, after only 1 h incubation. However, nearly

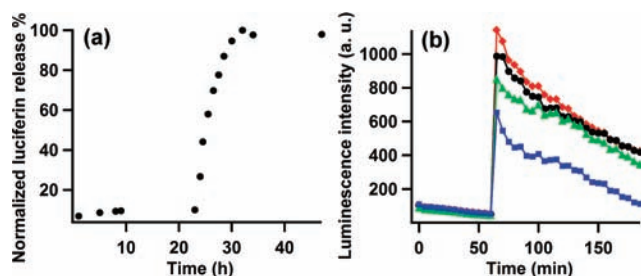


Figure 3. (a) Cumulative release of luciferin from a suspension of luciferin-loaded Au-MSNs (1 mg mL⁻¹) after addition of 1 mM DTT at 23 h. (b) Resultant luminescence from the luciferase–luciferin Au-MSN suspension (1 mg mL⁻¹) in the presence of ATP (80 μ M) and Mg²⁺ (8 mM) after the addition of (blue) 0.1, (green) 0.5, (red) 1, and (black) 10 mM DTT at 60 min.

75 and ~63% of the luciferase activity was observed after 3 h of contact with PEGylated linker-MSNs and PEG-AuNPs, respectively. The enzymatic activity of luciferase was also found to be dependent on the incubation time. A slight decrease in luciferase activity was found when the incubation time was increased from 3 to 24 h, in which nearly 60 and ~62% of the activity were observed for PEGylated linker-MSNs and PEG-AuNPs, respectively. These data demonstrate that surface PEGylation plays a crucial role in improving the biocompatibility of MSNs and AuNPs for the retention of enzyme bioactivity, which is consistent with other literature reports.^{22,28}

Having demonstrated the surface biocompatibility of the materials, we utilized the Au-MSN platform to adsorb and encapsulate the enzymatic substrate, luciferin. To do so, the mesopores of PEGylated linker-MSN (25 mg) were loaded with luciferin (33 μ M) in PBS buffer (pH 7.4) and then capped with PEG-AuNPs (25 mg) through amide bond formation between the carboxylic acid groups of PEG-AuNPs and the amino groups of PEGylated linker-MSNs (Figure 1), giving rise to the desired luciferin-loaded Au-MSNs (Figure 2b). The loading of luciferin was determined to be 13.1 μ mol g⁻¹ by fluorescence emission spectroscopy (see the SI).

TEM imaging provided visual evidence of the mesopore capping with PEG-AuNPs. Figure 2 shows TEM images of PEGylated linker-MSNs before and after capping with PEG-AuNPs. In the case of the uncapped MSN (Figure 2a), the hexagonally packed mesoporous channels are clearly visible. In contrast, the TEM image of a luciferin-loaded Au-MSN (Figure 2b) shows dark spots on the MSN surface that represent the attachment of AuNPs on the MSN exterior surface.

To determine whether the release of luciferin from the luciferin-loaded Au-MSNs could be induced by disulfide cleavage as desired for intracellular controlled release, luciferin-loaded Au-MSNs (1 mg mL⁻¹) were suspended in PBS buffer (pH 7.4) for 23 h before addition of 1 mM DTT. As shown in Figure 3a, the Au-MSN drug delivery system exhibited less than 5.0% drug release in PBS buffer over of the initial 23 h period. This result suggests a good capping efficiency of the AuNPs for encapsulation of the luciferin molecules against leaching. Addition of disulfide-reducing DTT (1 mM) triggered the release of the mesopore-entrapped luciferin. The rate of luciferin release slightly decreased over time until 100% of the total cumulative release (1.44 μ mol g⁻¹) was reached in 8 h. In addition, the controlled release of luciferin mediated by the Au-MSN system would offer the advantage of improving the circulatory half-life of luciferin

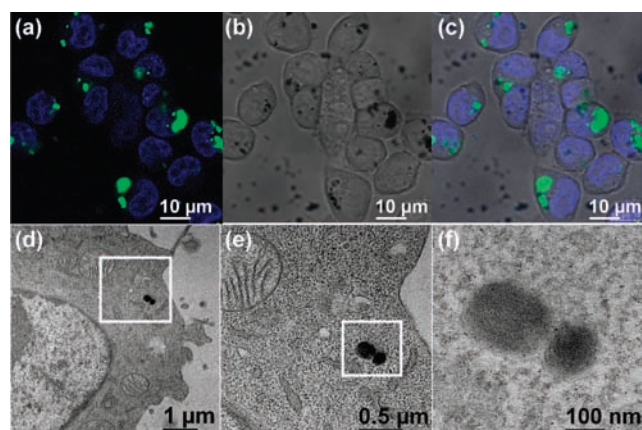


Figure 4. (a) Fluorescence confocal micrographs of HeLa cells (4×10^5 cells mL^{-1}) internalized with luciferase–luciferin FITC–Au–MSNs ($50 \mu\text{g mL}^{-1}$, green) for 3 h. Cell nuclei were stained with DAPI (blue). (b) Corresponding bright-field image of HeLa cells. (c) Fluorescence confocal and bright-field merged image. (d–f) TEM images of HeLa cells (4×10^5 cells mL^{-1}) internalized with luciferase–luciferin Au–MSNs ($50 \mu\text{g mL}^{-1}$) for 3 h. The images increase in magnification from left to right.

and also promote tumor uptake via the EPR effect, as required in various *in vitro* and *in vivo* luminescence assays. In addition, the disulfide linkage design renders the release of luciferin predominantly inside the cells.^{9,23,24}

The most advantageous feature of this Au–MSN platform is the potential to deliver different biogenic species simultaneously in a controlled fashion. To construct the enzyme–substrate codelivery system, luciferase was immobilized on the external surface of Au–MSNs by incubating luciferin-loaded Au–MSNs (1 mg mL^{-1}) with luciferase (1 mg mL^{-1}) in PBS buffer (pH 7.4) for 2 h, followed by centrifugation and freeze-drying. The loading of luciferase was measured to be $29.7 \mu\text{mol g}^{-1}$ by a luciferase activity assay (see the SI). This system will henceforth be called luciferase–luciferin Au–MSN. To examine the applicability of this controlled-release codelivery system, the DTT-stimulated luciferase–luciferin reaction was conducted *in situ* as described in the SI. The luminescence intensity remained at background level over a period of 60 min before the addition of disulfide-bond reducing agents, suggesting a “zero premature release” property of this system. After addition of DTT (1 mM), luciferase was released and converted to oxyluciferin in a luciferase-catalyzed light-emitting reaction. As shown in Figure 3b, the pattern of luminescence as a function of time was similar for all DTT doses (0.1, 0.5, 1, and 10 mM). The highest luminescence signal was detected at $t = 5$ min and gradually decayed, reaching background after ~ 180 min. The observed luminescence strongly depended on the DTT concentration. An increase in the luminescence signal was observed with growing DTT dose up to 1 mM, suggesting a dose-dependent controlled-release profile. Importantly, when 10 mM DTT was introduced to the system, the luminescence showed a 15% reduction in intensity relative to the signal triggered by 1 mM DTT, which can be attributed to the denaturation of luciferase at high DTT concentrations.²⁹ Hence, the effectiveness of the luciferase–luciferin reaction on the Au–MSN platform depends on the strength of the reducing environment to which it is exposed.

Prior to functional biological studies of the luciferase–luciferin Au–MSNs, it was necessary to evaluate the cellular uptake and cytotoxic effects of the material. To do so, we first assessed the

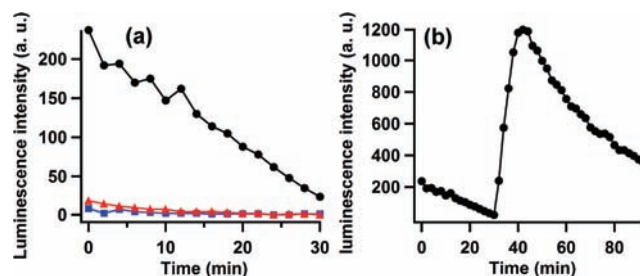


Figure 5. (a) Luminescence from HeLa cells (4×10^5 cells mL^{-1}) measured after 3 h of incubation with $50 \mu\text{g mL}^{-1}$ luciferase–luciferin Au–MSNs (black) or a solution containing free luciferase (1 mg mL^{-1}) and luciferin ($40 \mu\text{M}$) (red) compared with untreated cells (blue). (b) Observed luminescence of HeLa cells (4×10^5 cells mL^{-1}) after preincubation with luciferase–luciferin Au–MSNs ($50 \mu\text{g mL}^{-1}$) for 3 h; 1 mM DTT was added at $t = 30$ min.

cellular uptake of fluorescein isothiocyanate (FITC)-labeled luciferase–luciferin Au–MSNs (denoted as luciferase–luciferin FITC–Au–MSNs) by human cervical carcinoma (HeLa) cells over time. The cells were incubated in the presence of the NPs ($50 \mu\text{g mL}^{-1}$) for increasing periods of time. The percentage of cells internalizing luciferase–luciferin FITC–Au–MSNs was then monitored by flow cytometry using the trypan blue exclusion method for quenching the fluorescence of extracellular particles.³⁰ As shown in Figure S5, the percent of FITC-positive cells increased with time, reaching over 80% of total cellular uptake at 3 h of contact and a plateau in ~ 6 h. In view of the aforementioned incubation time effect on the luciferase activity (Figure S4), 3 h of contact was selected for the following biological experiments. We performed confocal fluorescence microscopy (Figure 4a–c) and TEM (Figure 4d–f) analyses of HeLa cells 3 h after treatment with $50 \mu\text{g mL}^{-1}$ luciferase–luciferin FITC–Au–MSNs and luciferase–luciferin Au–MSNs, respectively. Indeed, the nanoparticles were easily visible inside the cells, confirming uptake of the materials. Finally, the toxicity of the luciferase–luciferin Au–MSNs was assessed by Guava ViaCount cytometry assay with HeLa cells. Following 24 h of treatment, we observed minimal toxicity ($>95\%$ cell viability) at concentrations of the material as high as $100 \mu\text{g mL}^{-1}$ (Figure S6), consistent with the good biocompatibility of MSNs^{23,31} and AuNPs.³²

To demonstrate that the enzyme–substrate Au–MSN system can deliver both the enzyme luciferase and the substrate luciferin for intracellular ATP- and redox-potential-mediated biocatalysis, the luciferase–luciferin Au–MSNs ($50 \mu\text{g mL}^{-1}$) were internalized by HeLa cells. After 3 h of incubation, the intracellular luciferase-catalyzed luciferin conversion and light emission was assessed by means of an intracellular luciferase activity assay (see the SI). As shown in Figure 5a, a burst of luminescence was observed immediately and slowly decayed over the next 30 min. Neither untreated HeLa cells nor cells treated with a solution containing free luciferase and luciferin (10- and 15-fold relative to the loading amounts, respectively) generated detectable luminescence, consistent with the low extracellular ATP level^{33,34} and the membrane impermeability of luciferase.³⁵ Therefore, the observed luminescence can be attributed to the capability of our Au–MSN system for intracellular codelivery of enzyme and substrate. Furthermore, our model system provides a means of further regulating the enzymatic reaction inside live cells. As a first demonstration of intracellular catalysis with tunability, the enzymatic reaction efficiency was increased by enhancing the

intracellular reducing environment. As shown in Figure 5b, addition of 1 mM DTT after the decay of the initial intracellular disulfide-reducing antioxidant triggered luminescence that after 10 min reached a peak signal 5-fold higher than the highest initial luminescence and then gradually decayed, in accord with the in situ controlled-release experiment shown Figure 3b. Therefore, this system affords the possibility of serving as not only a universal enzyme–substrate carrier for intracellular controlled catalysis but also a unique reporter for monitoring the intracellular redox potential for the study of drug delivery, cell viability, and tumor growth.

In conclusion, the present study has introduced a novel approach to intracellular codelivery of enzyme and substrate that enables the system to be utilized in intracellular controlled catalysis. Although we have demonstrated only the codelivery of luciferase and luciferin in this study, the concept of delivering multiple biogenic agents using such systems could also be extended to other enzymatic reactions by exchanging the enzyme–substrate pair. In addition, it has been recently observed that MSNs are able to undergo exocytosis and harvest intracellular biomolecules,³⁶ and thus, we envision that our system could not only conduct biocatalysis inside live cells but also sequester the product out of cells for a variety of biotechnological applications.

The luciferase–luciferin Au-MSN system was designed to allow imaging and quantification of the intracellular catalysis for system optimization but also affords a unique route toward monitoring tumor growth and metastasis by means of bioluminescence and using intracellular ATP and GSH levels as indicators. In comparison with traditional bioluminescence assays, which generally employ gene engineering and multiple luciferin injections, only one system needs to be delivered in this strategy. Rapid readouts of the luminescence arising from NP internalization and the intracellular GSH-mediated luciferase–luciferin reaction provide a unique platform for evaluating tumor development and a convenient way of monitoring the response to treatments and measuring the therapeutic efficacy, which is of importance for medical diagnosis and drug screening and development.

■ ASSOCIATED CONTENT

S Supporting Information. Experimental details and characterization data. This material is available free of charge via the Internet at <http://pubs.acs.org>.

■ AUTHOR INFORMATION

Corresponding Author

islowing@iastate.edu; bgtrewyn@iastate.edu

Notes

[†]Deceased on May 4, 2010.

■ ACKNOWLEDGMENT

This work is dedicated to the memory of Dr. Victor Shang-Yi Lin. B.G.T., X.S., and Y.Z. thank the U.S. National Science Foundation (CHE-0809521) and I.I.S. thanks the Ames Laboratory, U.S. Department of Energy, Office of Basic Energy Sciences (Contract DE-AC02-07CH11358) for support to complete this project.

■ REFERENCES

- (1) Zhao, Y.; Vivero-Escoto, J. L.; Slowing, I. I.; Trewyn, B. G.; Lin, V. S.-Y. *Expert Opin. Drug Delivery* **2010**, *7*, 1013.
- (2) Slowing, I. I.; Trewyn, B. G.; Lin, V. S.-Y. *J. Am. Chem. Soc.* **2007**, *129*, 8845.
- (3) Bale, S. S.; Kwon, S. J.; Shah, D. A.; Banerjee, A.; Dordick, J. S.; Kane, R. S. *ACS Nano* **2010**, *4*, 1493.
- (4) Ghosh, P.; Yang, X.; Arvizo, R.; Zhu, Z.-J.; Agasti, S. S.; Mo, Z.; Rotello, V. M. *J. Am. Chem. Soc.* **2010**, *132*, 2642.
- (5) Bale, S. S.; Kwon, S. J.; Shah, D. A.; Kane, R. S.; Dordick, J. S. *Biotechnol. Bioeng.* **2010**, *107*, 1040.
- (6) Ahmann, F. R.; Garewal, H. S.; Schifman, R.; Celniker, A.; Rodney, S. *In Vitro Cell. Dev. Biol.* **1987**, *23*, 474.
- (7) Meyer, A. J.; Brach, T.; Marty, L.; Kreye, S.; Rouhier, N.; Jacquot, J.-P.; Hell, R. *Plant J.* **2007**, *52*, 973.
- (8) Balendiran, G. K.; Dabur, R.; Fraser, D. *Cell Biochem. Funct.* **2004**, *22*, 343.
- (9) Wu, G.; Fang, Y.-Z.; Yang, S.; Lupton, J. R.; Turner, N. D. *J. Nutr.* **2004**, *134*, 489.
- (10) Zhao, Y.; Trewyn, B. G.; Slowing, I. I.; Lin, V. S.-Y. *J. Am. Chem. Soc.* **2009**, *131*, 8398.
- (11) Torney, F.; Trewyn, B. G.; Lin, V. S.-Y.; Wang, K. *Nat. Nanotechnol.* **2007**, *2*, 295.
- (12) Sweeney, T. J.; Mailander, V.; Tucker, A. A.; Olomu, A. B.; Zhang, W.; Cao, Y.-A.; Negrin, R. S.; Contag, C. H. *Proc. Natl. Acad. Sci. U.S.A.* **1999**, *96*, 12044.
- (13) Jenkins, D. E.; Oei, Y.; Hornig, Y. S.; Yu, S.-F.; Dusich, J.; Purchio, T.; Contag, P. R. *Clin. Exp. Metastasis* **2003**, *20*, 733.
- (14) Liu, J. J.; Wang, W.; Dicker, D. T.; El-Deiry, W. S. *Cancer Biol. Ther.* **2005**, *4*, 885.
- (15) Chandran, S. S.; Williams, S. A.; Denmeade, S. R. *Luminescence* **2009**, *24*, 35.
- (16) Shinde, R.; Perkins, J.; Contag, C. H. *Biochemistry* **2006**, *45*, 11103.
- (17) Edinger, M.; Sweeney, T. J.; Tucker, A. A.; Olomu, A. B.; Negrin, R. S.; Contag, C. H. *Neoplasia* **1999**, *1*, 303.
- (18) Lundin, A.; Rickardsson, A.; Thore, A. *Anal. Biochem.* **1976**, *75*, 611.
- (19) DeLuca, M.; McElroy, W. D. *Biochemistry* **1974**, *13*, 921.
- (20) Berger, F.; Paulmurugan, R.; Bhaumik, S.; Gambhir Sanjiv, S. *Eur. J. Nucl. Med. Mol. Imaging* **2008**, *35*, 2275.
- (21) Matsumura, Y.; Maeda, H. *Cancer Res.* **1986**, *46*, 6387.
- (22) Hong, R.; Fischer, N. O.; Verma, A.; Goodman, C. M.; Emrick, T.; Rotello, V. M. *J. Am. Chem. Soc.* **2004**, *126*, 739.
- (23) Lai, C.-Y.; Trewyn, B. G.; Jeftinija, D. M.; Jeftinija, K.; Xu, S.; Jeftinija, S.; Lin, V. S.-Y. *J. Am. Chem. Soc.* **2003**, *125*, 4451.
- (24) Giri, S.; Trewyn, B. G.; Stellmaker, M. P.; Lin, V. S.-Y. *Angew. Chem., Int. Ed.* **2005**, *44*, 5038.
- (25) Brust, M.; Walker, M.; Bethell, D.; Schiffrin, D. J.; Whyman, R. *J. Chem. Soc., Chem. Commun.* **1994**, 801.
- (26) Leach, F. R.; Webster, J. J. *Methods Enzymol.* **1986**, *133*, 51.
- (27) Lin, S.; Cohen, H. P. *Anal. Biochem.* **1968**, *24*, 531.
- (28) Taluja, A.; Bae, Y. H. *Pharm. Res.* **2007**, *24*, 1517.
- (29) Lomakina, G. Y.; Modestova, Y. A.; Ugarova, N. N. *Vestn. Mosk. Univ., Ser. 2: Khim.* **2008**, *49*, 81.
- (30) Hed, J.; Hallden, G.; Johansson, S. G.; Larsson, P. *J. Immunol. Methods* **1987**, *101*, 119.
- (31) Slowing, I.; Trewyn, B. G.; Lin, V. S.-Y. *J. Am. Chem. Soc.* **2006**, *128*, 14792.
- (32) Arvizo, R.; Bhattacharya, R.; Mukherjee, P. *Expert Opin. Drug Delivery* **2010**, *7*, 753.
- (33) Gordon, J. L. *Biochem. J.* **1986**, *233*, 309.
- (34) Pellegatti, P.; Raffaghello, L.; Bianchi, G.; Piccardi, F.; Pistoia, V.; Di Virgilio, F. *PLoS One* **2008**, *3*, No. e2599.
- (35) Bayele, H. K.; Ramaswamy, C.; Wilderspin, A. F.; Srai, K. S.; Toth, I.; Florence, A. T. *J. Pharm. Sci.* **2006**, *95*, 1227.
- (36) Slowing, I. I.; Vivero-Escoto, J. L.; Zhao, Y.; Kandel, K.; Peerapatdit, C.; Trewyn, B. G.; Lin, V. S.-Y. *Small* **2011**, *7*, 1526.